

Memorandum

To: L3 Distribution
From: F. Primini
Subject: Recommendations for Estimating L3 Source Position Uncertainties
Date:

1) Introduction

In this memo I describe the simulation procedures I used to evaluate L3 *wavdetect* positional uncertainties, the simulation results, and the evidence I've found for non-circular error distributions. I also specify how to use *ChaMP* empirical relations to estimate position uncertainties for L3.

2) Simulation Procedure

ChaRT was used to generate a library of ray-traces for a number of off-axis angles and azimuths, as detailed in the following table.

θ (')	ϕ (°)	Energy (keV)	Ray Density (rays/mm ²)
0	0	2.36	5
1	Every 30 starting at 0	2.36	5
5	Every 30 starting at 0	2.36	5
7.5	45, 135, 225, 315	2.36	5
9.5	45, 135, 225, 315	2.36	5
15	112.5	2.36	10
18.5	113.5	2.36	10

The energy was chosen to approximate the effective energy for the L3 broad band.

The ray-traces were then projected to detector and sky coordinates for OBSID 2925, an ACIS-I observation in which ACIS-S chips S2 and S3 were also included (the rather unusual choices for θ, ϕ for large off-axis angle sources were chosen to ensure valid detector coordinates for this observation). The simulated event lists contained fields `ccd_id`, `chip`, `det`, sky coordinates, and energy.

For each simulation run, 100 events were randomly selected from the appropriate simulated event lists and appended to a version of the L3 event list for OBSID 2925 that had been filtered to include the same fields as the simulated event lists. An example is shown in Figure 1. The resulting event list, plus all associated data products, were then input to the CAT2.4 versions of the L3 detect pipeline, namely, `lev3_make_image.sl`, `lev3_run_wavdetect.sl`, `lev3_filter_srcs.sl`, and `merge_src`, using standard L3 parameters. Approximately 100 simulations were run for each value of off-axis angle.

The outputs from `merge_src` were collected and concatenated into a single table, whose source positions were cross-referenced to a table of positions for the simulated sources. This latter table was obtained by converting from `theta,phi` to sky coordinates using `dmcoords`, with the original OBSID 2925 event list as a reference file. Offsets in `x` and `y` between the detected simulated

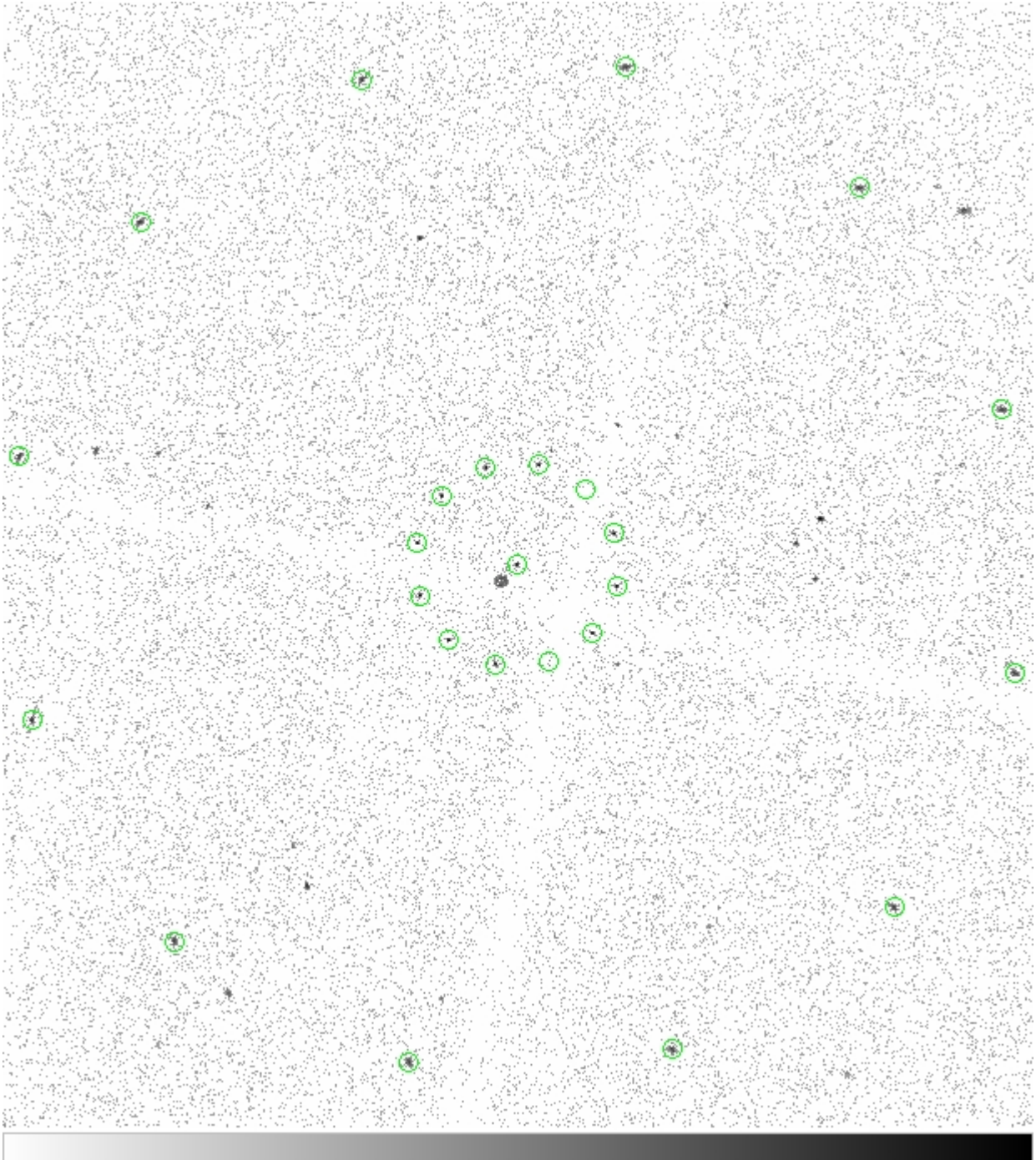


Figure 1: L3 event list with simulated sources at $\theta=0'$, $1'$, and $5'$

source positions and their reference positions were then computed and tabulated.

3) Simulation Results

For the initial evaluation, the azimuthal dependence was ignored, and the dependence of radial offsets (i.e., the quadrature sums of x and y offsets between detected and reference positions) on off-axis angle was compared to the run of *wavdetect*-reported position errors vs. off-axis

angle from the earlier test runs of 100 and 200 OBSIDs, and also to the predicted *ChaMP* relation (Kim et al. 2007, ApJS, 169, 401). Results are shown in Figure 2.

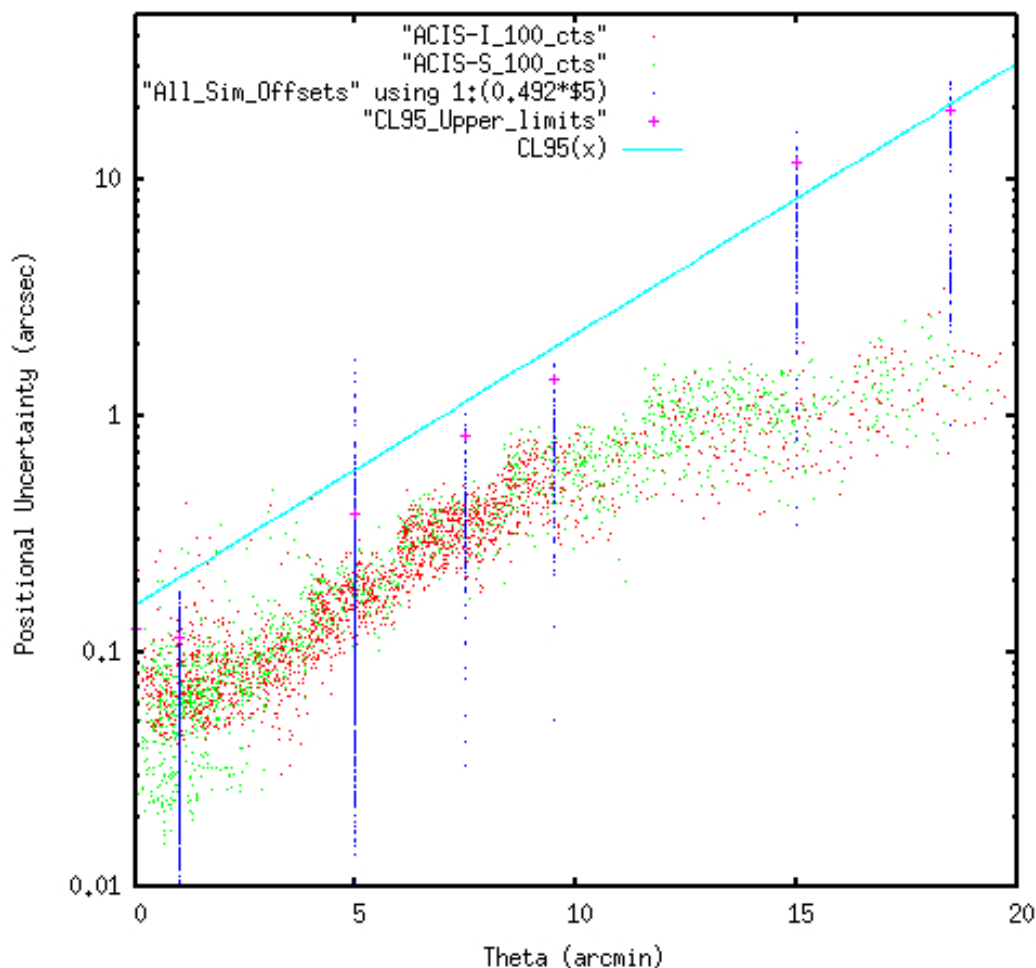


Figure 2: Positional uncertainties vs. theta for simulated sources (blue), *wavdetect* sources (red and green) and *ChaMP* (cyan curve). Points labeled “CL95 Upper Limits” are the 95% quantiles of the distributions of radial offsets at each value of theta.

In this plot, the *ChaMP* curve represents the 95% Confidence Level errors (as recommended by D.-W. Kim) for a 100 count source, the *wavdetect* errors were selected from sources with 50-150 net counts reported by the program, and all simulated source offsets are plotted.

As demonstrated in Figure 2, our limited simulations are roughly consistent with the more extensive *ChaMP* simulations and both indicate that *wavdetect*-reported errors underestimate actual errors for large values of theta.

Of course, the limited L3 simulations are not sufficient to fully characterize the positional uncertainties. Only a single OBSID (and hence background level) was used, and sources of only a single intensity were simulated, in a rather sparse theta,phi grid. Moreover, the *ChaMP* and L3 simulation results, while similar, appear to differ in the values of the coefficients of PU vs. theta. Finally, only broad band PSFs were simulated, and it's possible that the coefficients would depend on energy band. The current simulations can only be considered a “spot-check” of the *ChaMP* results, and more extensive simulations should be carried out to explore the above issues. However, given the extensive *ChaMP* simulations and the general agreement, I recommend that we adopt the *ChaMP* relation for now, and carry out more extensive L3 simulations on a timescale that does not impact the near-term schedule.

4) Evidence for Non-Circular Errors

The above analysis ignored any dependence of positional uncertainties on azimuthal angle (ϕ). One can search for an azimuthal dependence by examining individual x and y offsets between detected and reference positions of simulated sources for a single value of both θ and ϕ . Sample results are shown in Figure 3. These results indicate that it may in fact be possible to derive elliptical error regions from our simulations. One would need to determine the best ellipse (according to some as yet unspecified metric) which enclosed 95% of the simulated offsets.

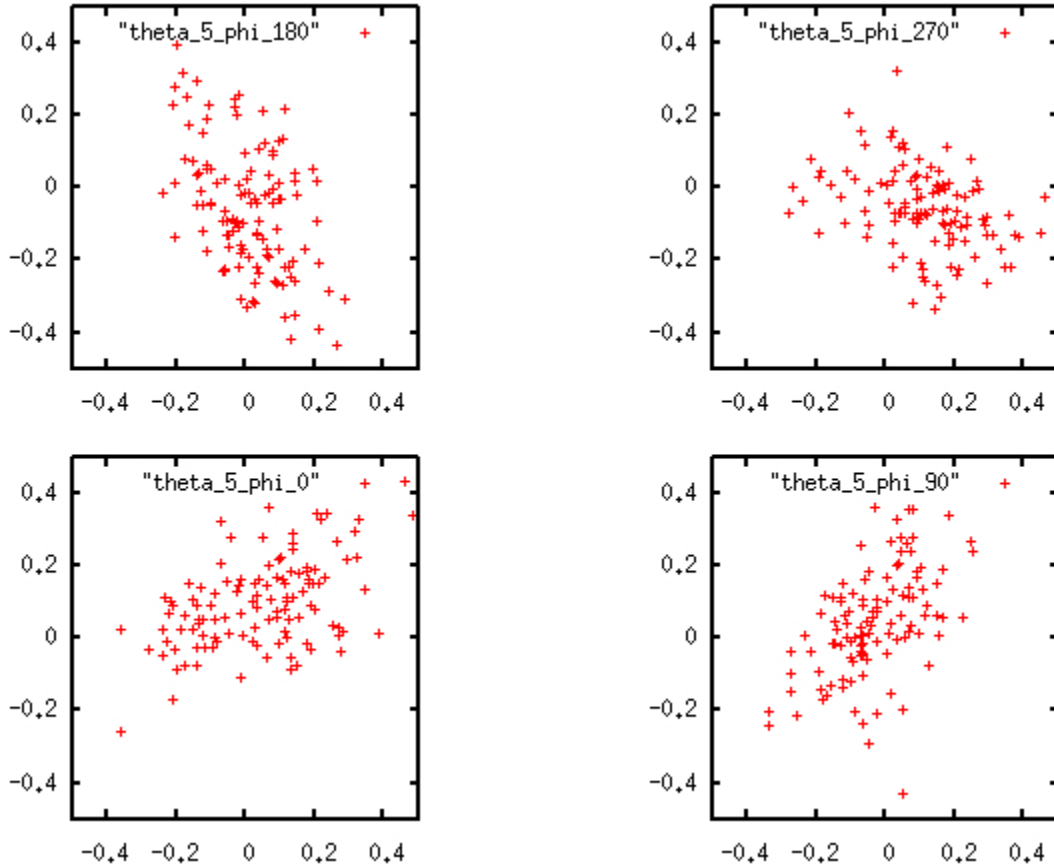


Figure 3: X offset vs. Y offset from reference source position for 4 values of azimuthal angle $\phi=0, 90, 180,$ and 270 degrees, and $\theta=5'$

However, this would involve many more simulations to provide a sufficiently dense grid in θ and ϕ . These should be included in the additional simulations discussed above.

5) Implementation of ChaMP Positional Uncertainties

It remains only to specify how to use the *ChaMP* relation. I recommend that we use the relation for the 95% Confidence Level error circles (Eq. 12, Kim et al. 2007), namely

$$\log PU = 0.1145\theta - 0.4958\log(\text{net counts}) + 0.1932 \quad 0 < \log(\text{net counts}) \leq 2.1393 \quad (1)$$

$$\log PU = 0.0968\theta - 0.2064\log(\text{net counts}) - 0.4260 \quad 2.1393 < \log(\text{net counts}) \leq 3.3 \quad (2)$$

Here, *net counts* are those reported by *wavdetect* (that's what *ChaMP* used to calibrate the relation). For sources brighter than $\log(\text{net counts})=3.3$, I recommend that we use equation 2. To account for the possibility that L3 coefficients may differ from *ChaMP* values, all the coefficients

in equations 1 and 2 should be kept as parameters in an L3 parameter file. Moreover, separate parameter sets should be maintained for each energy band, although (for now) the actual values will be the same for all bands. The specification for computing position errors is then:

1. For each source in the merge_src3.fits file, determine θ and *net counts*. When sources are detected in multiple bands or blocking factors, use the *net counts* from the band/block that survives the merging process (i.e., the “best” source).
2. Compute *PU* from either equation 1 or 2, depending on the value of *net counts*.
3. Set the source position error ellipse semi-major and semi-minor axis values to *PU*.
4. Set the source position error ellipse position angle to 0.